Physical and Optical Properties of Rare Earth Cobalt Magnets

Klaus Halbach

Lawrence Berkeley Laboratory, UC Berkeley,
Berkeley, CA. 94720

Rare Earth Cobalt (REC) permanent magnets have unique properties that permit solutions to some optical tasks that cannot be accomplished with conventional magnets. A review of design and of performance characteristics of these magnets includes an analytical description of the three dimensional fringe fields of REC quadrupoles.

1) Introduction

There are indications that Rare Earth Cobalt (REC) permanent magnets will soon be used much more frequently to solve optical problems that cannot be solved with conventional means. It is the purpose of this paper to summarize information that is useful for the design of REC magnets and to assess their performance characteristics. The optical properties of the devices discussed here usually can be obtained directly and very simply from the magnetic field distributions. The emphasis is therefore on the description of the latter, the former following in most cases directly by implication.

Since REC magnets have not yet been used extensively, the choice of devices that are discussed in detail reflects my expectation of which kind of REC magnet will become important in the near future.

Design and performance formulas are given to allow the reader to make a decision whether a REC device is a good choice for his needs. The specific designs of magnets that are discussed represent a good compromise between performance and cost for most applications. If the reader wants to work out more details of a particular magnet, he may find Ref. 1 useful. That paper gives general design philosophy and procedures for the design of REC magnets, and extensive details about the design of two dimensional (2D) multipoles. Quantitative details about the fringe fields of quadrupoles as well as a description of the other devices discussed in this paper will appear in future publications by the author.

2) Notation

MKS units are used throughout, with $\mu_0 = 4\pi \times 10^{-7}$ Vsec A^{-1} m^{-1}. For 2D fields it is convenient to express fields by analytical functions of a complex variable. Complex quantities are identified by underlining. Specifically, z is one of the three space coordinates, but $\underline{z} = x + iy$. 2D fields are described by $\underline{B} = B_x + iB_y$, with an asterisk* indicating the complex conjugate of a complex number. B_r indicates the magnitude of the remanent magnetization of the material, and $\underline{B}_r$ is the 2D remanent magnetization vector.

3) Material Properties

The development of REC materials started in 1966 with Strnat's[2] work. Brief summaries of the manufacturing process can be found in References 1 and 3, while Ref. 4 goes into detail. We give here only a brief description of the properties of commercially available REC.

Oriented REC material is a magnetically anisotropic material with a strong intrinsic magnetization in the direction of a preferred crystalline axis, commonly called the easy axis. Fig. 1 shows the relationship between the fields $B_{//}$ and $\mu_0 H_{//}$ in the direction parallel to that easy axis. This $B_{//}(\mu_0 H_{//})$-curve is, for all intents and purposes, a straight line in the first quadrant and in a substantial part of the second, or even third, quadrant. The slope of the curve in the straight part of the curve is typically $dB_{//}/d(\mu_0 H_{//}) = 1.04$, and the remanent field B_r is usually in the range .85 - 1.05T. The location of the point where the slope of the $B_{//}(\mu_0 H_{//})$-curve increases significantly, i.e., the knee of the $B_{//}(\mu_0 H_{//})$-curve, depends on manufacturing details and cannot be modified by the user. For readily available materials, the knee is located less deeply in the second or third quadrant for larger values of B_r. The working point can be moved reversibly along the straight part of the $B_{//}(\mu_0 H_{//})$-curve, but when one moves into or beyond the knee, the recoil will occur along a straight line parallel to the initial straight part of the $B_{//}(\mu_0 H_{//})$-curve, and the initial magnetization can be recovered only by driving the material very far into the first quadrant.

The $B_{\perp}(\mu_0 H_{\perp})$-curve in any direction perpendicular to the easy axis is a straight line through the origin $B_{\perp} = \mu_0 H_{\perp} = 0$, with a slope very similar to the slope of the $B_{//}(\mu_0 H_{//})$-curve. All formulas given in this paper have been derived with the simplifying assumption that the slopes of both curves are one. The most important consequence of this assumption is the applicability of the linear superposition of vacuum fields. In real life, this assumption is violated only very slightly, particularly because the most damaging deviations from vacuum fields are sensitive only to the difference in differential permeability in the directions parallel and perpendicular to the easy axis.

For the sake of completeness, it should be pointed out that some ferrites behave qualitatively similar to REC, but are quantitatively different: the differential permeabilities are ≥ 1.1 and B_r is only .2 - .35 T.

It is difficult to talk about the price of finished pieces of magnetized REC because many different variables enter, like magnetic characteristics of the material, size and shape of pieces, tolerances of dimensions and magnetic properties, total volume of order, etc. But to give a rough guideline for pricing, it can be said that most commercial orders will cost between 1.5 and 30 $/cm^3. Ferrites are substantially less expensive.

4) General Properties of REC Magnets for Particle Optics Applications

This section presents a number of facts that are applicable to all REC magnets. These facts are often compared with equivalent properties of conventional magnets to give an indication under what circumstances the REC magnet would be preferable.

A. When one scales all dimensions of a permanent magnet, the magnetic fields do not change. When one reduces the size of a conventional magnet and wants the fields to remain constant, the current density in the coils must increase. At some size this will lead to insurmountable cooling problems that force a reduction of the field strength. Consequently, a REC magnet can always produce higher fields below a certain size of the magnet or working volume. To avoid a misinterpretation of this statement, it has to be added that for some types of magnets, the REC magnet can be made stronger than the equivalent conventional magnet, regardless of size.

B. REC magnets are usually quite compact and light, and obviously do not require power supplies or cooling. These properties are of great importance in some applications, like drift tube quadrupoles in a LINAC, or spectrometers in satellites or rockets.

C. The absence of power supply leads and plumbing associated with either conventional or He cooling makes REC magnets very attractive for some applications, for example a variable gap undulator inside a vacuum envelope.

D. The applicability of linear superposition of magnetic fields makes analytical description of REC magnets very easy. I consider this quite important because analytical treatment nearly always leads to good understanding, from which good design and innovation nearly always flow. The validity of linear superposition of fields also leads to a number of remarkable and unusual configurations and system properties, some of which are discussed below in subsections E and F.

E. REC magnets can be placed inside other magnets, with linear superposition of fields in the common working volume, and very little magnetic interference in the rest of the magnetic field volume. Typical anticipated applications are: a) A strong final focussing REC quadrupole inside the solenoid of a storage ring or single pass collider interaction region detector. b) A REC undulator with weak quadrupole windings. c) A REC quadrupole inside the working volume of another REC quadrupole, giving a variable strength quadrupole when the two quadrupoles are rotated relative to each other.

F. Because of the superposition principle, most pure REC magnets produce fields that are very small outside the working volume as well as the magnet itself, and decay there over very short distances.

G. There is not very much known about the behaviour of REC magnets in a high radiation environment. Materials experts do not believe that the magnetic properties deteriorate easily. Some preliminary work confirms this, and detailed work will commence in the near future.

H. REC magnets can easily be taken to 200°C, and even higher temperatures if proper precautions are taken. However, the temperature should always be fairly uniform and, for that reason, should not be changed too rapidly.

I. With the presently most widely used manufacturing techniques, the smallest dimension of a REC block cannot be larger than a few centimeters. Even though magnets can be (and are) assembled from many blocks, devices involving large volumes of REC become very expensive

because of the material costs and the labor costs involved in making and handling a very large number of individual components.

5) Multipole Magnets

To produce a strong 2D multipole with good field quality (i.e., a REC magnet with $B^* \sim z^{N-1}$) the REC ideally should fill the area between two concentric circles, and the easy axis of the material at the polar coordinate location r, ϕ should form the angle

$$\beta(\phi) = (N+1) \cdot \phi \qquad (1)$$

with the $\phi = 0$ direction.

Since it would be very difficult to produce such a magnet, one has to make a compromise between performance and cost of the magnet. The following practical design is such a compromise: Break up the material between the concentric circles into M geometrically identical blocks. Within each block the easy axis has the same orientation, and that orientation is given by eqn. (1), with ϕ now identifying a fiducial mark on the block. Fig. 2 shows a schematic cross-section of such a multipole magnet (in this case a quadrupole, i.e., N = 2), with the arrows inside the blocks indicating the directions of the easy axes.

If the individual blocks are touching trapezoids, the 2D fields produced by a 2N-pole magnet inside the working aperture is given by

$$\left.\begin{aligned} \underline{B}^*(z_0) &= \underline{B}_r \sum_{\nu=0} \left(\frac{z_0}{r_1}\right)^{n-1} \cdot \frac{n}{n-1} \cdot \left[1 - \left(\frac{r_1}{r_2}\right)^{n-1}\right] \cdot C_n \\ n &= N + \nu \cdot M \\ C_n &= \cos^n(\pi/M) \cdot \sin(n\pi/M)/(n\pi/M) \\ \left(\frac{n}{n-1}\left[1 - \left(\frac{r_1}{r_2}\right)^{n-1}\right]\right)_{n\to 1} &= \ln(r_2/r_1) \end{aligned}\right\} \qquad (2)$$

$\underline{B}_r$ is the complex representation of the magnetization vector of the reference trapezoidal block that is bisected by the positive x-axis; r_1 and r_2 are the distances between the coordinate origin and the intersections between the reference block and the positive x-axis; and M is the number of trapezoidal blocks per magnet. Ref. 1 gives also the formulas for multipoles with differently shaped or arranged blocks. They are structurally identical to Eqn. (2), but with different expressions C_n.

The fields outside such a magnet are given by

$$\left.\begin{aligned} \underline{B}^{*}(z_0) &= \underline{B}_r \sum_{\nu=1} \left(\frac{r_2}{\underline{z}_0}\right)^{n+1} \cdot \frac{n}{n+1} \cdot \left[1-\left(\frac{r_1}{r_2}\right)^{n+1}\right] \cdot C_{-n} \\ n &= \nu \cdot M - N \\ C_{-n} &= \cos^{-n}(\pi/M) \cdot \sin(n\pi/M)/(n\pi/M) \end{aligned}\right\} \quad (3)$$

From Eqn's. (2) and (3) follow three important facts:

A. The segmentation of the magnet, i.e., the finite magnitude of M, leads to a reduced magnetic field (expressed by C_n) and to harmonics that may be harmful. For a quadrupole (N = 2) with M = 16, C_2 = .94 and the first two undesired harmonics are n = 18 and n = 34. Clearly, C_2 is adequately close to the ideal value 1. In the unlikely case that the first undesired harmonic is bothersome, its amplitude can be made zero by separating the REC blocks by thin non-magnetic shims according to a prescription given in Ref. 1.

B. The segmentation of the multipole leads also to non-zero fields outside the magnet. However, for reasonably large values of M these fields are so small and decay so rapidly that they are rarely of concern.

C. The field strength of the fundamental at the multipole aperture

$$\left(B_r \cdot \frac{N}{N-1} \cdot \left[1-\left(\frac{r_1}{r_2}\right)^{N-1}\right] C_N\right)$$ can, for low order multipoles like dipoles and quadrupoles, exceed B_r significantly. It has to be remembered that this field strength is attained only if the material under these operating conditions is not driven into or beyond the knee of the $B_{//}$ ($\mu_0 H_{//}$)-curve. Some materials are commercially available that allow aperture fields of 1.2 T.

In addition, if the ends of a multipole are cut off with two planes perpendicular to the magnet axis, the following statements are true:

D. The effective magnetic length equals its physical length.

E. Higher harmonics that are not present in the 2D cross-section are not present in the fringe field region either. In this context, higher harmonics are identified by the dependence of fields or potentials on ϕ.

6) Additional Details for Quadrupoles and Dipoles.

A. If one replaces all REC inside a closed scalar potential surface by high permeability steel, the performance of the magnet will not be affected as long as the permeability of the steel is large enough. One can find such closed scalar potential surfaces for multipoles, but the savings in REC materials cost is usually not worth the complication in construction, except possibly for a dipole. When a dipole is needed with a working volume whose

cross-section much wider than it is high, this technique can lead to a rather attractive design. However, detailed design studies and comparison with conventional combined REC-steel magnet designs have not yet been done.

B. Quadrupoles of the basic design shown in Fig. 2 have been built in large numbers by R. F. Holsinger. They have all the expected properties. Details of design and measurements of these quadrupoles can be found in Ref. 5 and 6.

C. It is often desirable to adjust the strength of quadrupoles. This can be done in at least three different ways with steel-free REC magnets. a) As mentioned in Sect. 4Ec, one segmented quadrupole (or a quadrupole assembled from rods of circular cross-section, as proposed in Ref. 7) could be placed inside the working volume of a larger quadrupole of the same design. If both quadrupoles produce the same field gradient, the combined gradient can be changed without changing the quadrupole field orientation if the two quadrupoles are rotated by the same amount in opposite directions. However, since the end-fringe fields from the two quadrupoles behave differently, the fields in the end regions will change direction. (See Sect. 6 D.) This in turn will lead to some optical coupling between the usually decoupled two major planes of a quadrupole. b) To avoid this drawback, one can build a segmented quadrupole with radially movable segments. The trouble with this design is its mechanical complexity. c) One can also break up a quadrupole into a number of axial "slices" and rotate them individually in such a manner that the optical strength of the system is modified without introducing the coupling associated with the method described in Sect. 6 Ca. R. L. Gluckstern has studied this problem, found a solution, and will present it at this Conference[8].

D. The fringe field of a quadrupole can be of interest for a number of reasons, for instance to assess the coupling introduced by an adjustable quadrupole system of the kind described in Sect. 6 Ca, or to obtain information about optical aberrations. Since the higher harmonics are usually of such high order that their contribution to the fringe fields is of no interest, only the fringe field of the fundamental is described here. The configuration considered here is a semi-infinite quadrupole with a flatly cut end, as shown in Fig. 3. The fringe field can be derived from the scalar potential V(x, y, z), given by the following equations:

$$V(x,y,z) = B_r \cdot C_2 \cdot \left(\frac{1}{r_1} - \frac{1}{r_2}\right) \cdot (x^2 - y^2) \cdot L_2\left[(x^2+y^2)\cdot\frac{\partial^2}{\partial z^2}\right] \cdot F(z) \qquad (4a)$$

$$L_2(u) = \sum_{\nu=0}^{\infty} \frac{2\cdot(-u/4)^\nu}{\nu!\,(\nu+2)!} = 1 - \frac{u}{12} + - \cdots \qquad (4b)$$

$$v_2 = 1/\sqrt{1+(z/r_2)^2} \qquad (4c)$$

$$F(z) = \frac{1}{2}\cdot\left(1 - \frac{\frac{1}{r_1}+\frac{1}{r_2}}{8}\cdot z \cdot \frac{v_1^2 v_2^2 (v_1^2 + v_1 v_2 + v_2^2 + 4 + 8/v_1 v_2)}{v_1 + v_2}\right) \qquad (4d)$$

$$F''(z) = \frac{3}{8}\,\frac{\left(\frac{1}{r_1}-\frac{1}{r_2}\right)^{-1}}{z^3}\left(\left(1+\frac{\gamma}{2}z^2/r_2^2\right)v_2^{\gamma}-\left(1+\frac{\gamma}{2}z^2/r_1^2\right)v_1^{\gamma}\right) \qquad (4e)$$

These formulas are valid when the quadrupole segments fill the space between two circles with radii r_1 and r_2 completely. In this case,

$$C_1 = \sin(3\pi/M)/(3\pi/M) \; . \qquad (4f)$$

However, if M is reasonably large, Eqn's. (4) adequately describe the case of a quadrupole assembled from trapezoidal blocks.

Notice that the coordinate system used here is rotated by 45° relative to the system normally used to describe quadrupoles.

F"(z) (Eqn. 4e) describes the strength of the lowest order aberration associated with the varying quadrupole strength. Plots of F and F" are reproduced in Figures 4 and 5 for $z \geq 0$. The values of F and F" for $z < 0$ follow from the obvious symmetry properties of F and F". If one expands F for $z \gg r_2$, the dominant term is given by

$$F = \frac{1}{32}\cdot\frac{r_2^5 - r_1^5}{r_2 - r_1}\cdot\frac{r_1 r_2}{z^6} \; , \qquad (4g)$$

indicating a pleasantly fast decay.

Of the many different uses of Eqn's. (4), one deserves special notice. The integrals involved for calculation of the kick received by a particle going in a straight line through the fringe field region are very simple, and one obtains, with B' = field gradient deep inside the quadrupole:

$$\int_{-\infty}^{\infty} \Delta B_x \, dz = \frac{B'}{6}\int_{-\infty}^{\infty}(x_0 + x_0' z)^3 \cdot F''(z)\, dz = B'\cdot\left(x_0^2 x_0'/2 + x_0'^3 r_1 r_2/8\right) \qquad (4h)$$

In this equation, the genesis of the existing and non-existing terms is as follows: a term proportional to x_0^3 is always absent; the term proportional to x_0 is absent because $F''(-z) = -F''(z)$; the coefficient of the term proportional to x_0' is independant of the detailed behavior of

F(z); only the coefficient of the term proportional to $x_0'^3$ depends on the shape of F(z).

7) Linear Undulators

Linear undulators can be essential components of free electron lasers, and can be used to produce synchrotron radiation from an electron beam, or even a proton beam (for beam diagnostics[9] purposes). Under some circumstances, REC undulators are preferable to conventional ones, and Ref. 10 describes the use of a REC undulator in an optical clystron, but without giving any of the undulator design details.

Fig. 6 shows a schematic cross-section of a linear undulator with period length λ and M' = 4 blocks of REC per period in each half of the undulator. If the undulator is long enough in the direction perpendicular to the paper plane, the purely 2D field inside the undulator (i.e., $-h < y < h$) is given by

$$\underline{B}^*(z) = i \cdot 2 \cdot B_r \cdot \sum_{\nu=0} \cos(n k z) \cdot e^{-nkh} \cdot \left(1 - e^{-nkL}\right) \sin(n\varepsilon\pi/M') / (n\bar{\nu}/M') \Big\} \quad (5)$$

$$n = 1 + \nu \cdot M' \quad ; \quad k = 2\pi/\lambda$$

It has been assumed that from each block to the next, the easy axis is rotated by $2\pi/M'$.

The structure of this equation is very similar to the structure of the equation describing the field of a segmented multipole: Because of the segmentation, there are harmonics present; as in the case of multipoles, the harmonics corresponding to negative n lead to fields outside the device (i.e., $|y| > h + L$), but are not given here. For most practical values of kh, the higher harmonics are not of great importance. The first of the harmonics can be cancelled by using $\varepsilon = 1/(1 + 1/M')$. However, there is a loss of amplitude of the fundamental involved (which can be reduced with a more complicated shape of the blocks), so that one would use this procedure only when absolutely necessary.

If one ignores the synchrotron radiation effects, the effect of the undulator fields on particle trajectories is, to lowest order in $(B_{max}/k)/(p/e)$ (B_{max} = maximum field for y = 0; p and e are momentum and charge of the particle), as follows: in the z direction, the device acts for all intents and purposes like a pure drift space, and the motion in the y direction is governed by

$$y'' + y \cdot (B_{max} e/p)^2/2 = 0.$$

Eqn. (5) shows the same hard limit on the achievable field strength that charaterizes all pure REC magnets: for given geometric parameters, the obtainable field strength is limited by the properties of the REC material. For this reason, high field undulators with large gaps and period lengths should be built with conventional technology. However, for most of the presently interesting combinations of geometric parameters and field strength, the REC undulator is the ideal solution. If one wishes to have an undulator

with a small period length and a higher field than is obtainable with a REC undulator, one has to consider a superconducting undulator. Unfortuantely, the cost and operational complexity of such a device are often so prohibitive that one has to be content with the performance of the REC undulator.

It is often important to adjust the fields at the entrance and exit of the undulator in such a way that the total flux traversed by the beam is zero and a field symmetry condition is accurately satisfied. These adjustments can be done either by mechanically rotating REC blocks at the ends or by energizing tuning coils. These systems are too specific to be included here.

In the construction of an undulator it is important to make the device long enough in the z direction of Fig. 6 so that the finite length of the device does not modify significantly the 2D fields seen by the beam. On the other hand, for cost and other reasons one does not want to make the undulator wider than necessary.

To provide the information needed to determine the proper width of an undulator, the following Eqn's. (6) can be used to evaluate B_y in the midplane of a semi-infinite undulator (as shown in Fig. 7), thereby permitting the calculation of the effect of the "missing" parts of an undulator of infinite width.

$$\beta_1 = k\,h;\quad \beta_2 = k(h+L);\quad \gamma = kz;\quad \rho = \sqrt{\beta^2+\gamma^2} \qquad (6a)$$

$$\delta = \gamma\cdot\left(\sqrt{1+\gamma^2/\beta^2}+1\right)^{-1/2}/\beta \qquad (6b)$$

$$B_0 = 2\cdot B_r\cdot \sin(\xi\pi/M')/(\pi/M') \qquad (6c)$$

$$B_y(z) = B_0\cdot\left(U(\beta_1,\gamma)-U(\beta_2,\gamma)\right) \qquad (6d)$$

$$U(\beta,\gamma) = e^{-\rho}\cdot\left(\sqrt{1+\gamma^2/\beta^2}+1\right)^{1/2}\cdot W(\beta,\gamma) \qquad (6e)$$

$$W(\beta,\gamma) = \frac{1}{\pi}\cdot\int_0^{x_1}\frac{\exp(-\rho u/(1-u))}{\sqrt{2-u}}\cdot\frac{dx}{1+2x(x-1)} \qquad (6f)$$

$$u = \left(\delta\cdot x/(x-1)\right)^2;\quad x_1 = 1/(1+\delta) \qquad (6g)$$

Information for $\gamma < 0$ is obtainable from the behaviour for $\gamma > 0$ through

$$U(\beta,-\gamma) = e^{-\rho}-U(\beta,\gamma) \qquad (6h)$$

The "output" information is obtained from Eqn. (6d), with Eqn's. (6e) and (6f) providing the essential input for Eqn. (6d). Instead of a graph of $U(\beta,\gamma)$, Fig. 8 shows the less violently changing function $U(\beta,\gamma)\cdot e^{p}$.

8. Helical Undulator

Under some circumstances it is more advantageous to use a helical undulator, i.e., a device that produces a field that has on axis a dipole component in the direction perpendicular to the axis, with the direction of that field changing uniformly as one moves along the axis uniformly.

To implement such an undulator with REC, one can build short (in the z-direction) segmented dipoles, and rotate each short dipole relative to the previous dipole so that one obtains the desired period length λ in the z direction. If there are N' such slices per period λ, one obtains for the strength, on axis, of this REC undulator

$$B = B_r \cdot C_1 \cdot \frac{\sin \pi/N'}{\pi/N'} \cdot (T(x_1) - T(x_2)) \tag{7a}$$

$$T(x) = K_0(x) \cdot \frac{x}{2} \cdot K_1(x) \tag{7b}$$

$$x = 2\pi r/\lambda \ . \tag{7c}$$

Eqn. (7a) is valid for the case where the segments fill the space between two circles with radii r_1 and r_2 completely, and

$$C_1 = \frac{\sin 2\pi/M}{2\pi/M} \ , \tag{7d}$$

with M = number of segments in a dipole slice. However, these equations can be applied to the design with trapezoidal segments with very little error when M is reasonably large.

K_0 and K_1 in Eqn. (7b) are modified Bessel functions, and a graphic representation of $\ln(T(x))$ is reproduced in Fig. 9.

9) Production of Solenoidal Fields with REC

It is clear that some properties of fields produced by solenoids are impossible to reproduce with REC structures. The most obvious condition that is always satisfied by REC devices that produce fields of the same symmetry as solenoids is

$$\int_{-\infty}^{\infty} B_z(z)dz = 0. \tag{8}$$

While the same integral is in general not zero when solenoids produce the fields, Eqn. (8) is not a severe restriction under many circumstances, since matrix elements m(z) of the first order optical transfer matrices of a beam travelling along the axis satisfy the differential equation

$$m(z)'' + K^2 \cdot m(z) = 0 \qquad (9)$$

$$K(z) = \frac{B_z(z)}{2p/e}$$

In Eqn. (9), p and e are momentum and charge of the particle, and it is assumed that the matrix is expressed in a coordinate system that is rotated by

$$\alpha(z) = -\int_{z_{start}}^{z} K(z)dz \qquad (10)$$

relative to its orientation at the starting point. Since it is K^2 that appears in Eqn. (9), the sign reversals of $B_z(z)$ are usually not of major importance.

To give a feeling of what one can accomplish with REC, consider a segmented periodic array of magnetized REC rings, as shown in Fig. 10. With M' rings per period λ, and an easy axis rotation of $2\pi/M'$ from one ring to the next, one obtains for the scalar potential

$$V = -B_r \cdot \sum_{\nu=0} \frac{\sin(nkz)}{nk} \cdot I_0(kr) \cdot (G(nk_1) - G(nk_2)) \cdot \frac{\sin n\pi/M'}{n\pi/M'} \quad , \qquad (11a)$$

and for the field on axis

$$B_z(z) = B_r \cdot \sum_{\nu=0} \cos(nkz) \cdot (G(nx_1) - G(nx_2)) \cdot \sin(n\pi/M')/(n\pi/M') \qquad (11b)$$

$$n = 1 + \nu \cdot M' \; ; \; k = 2\pi/\lambda \; ; \; x_1 = kr_1 \; ; \; x_2 = kr_2 \qquad (11c)$$

$$G(x) = x \cdot K_1(x) + K_0(x) + \int_x^\infty K_0(x)\,dx \qquad (11d)$$

In Eqn's. (11a) and (11d), I_0, K_0, and K_1 are modified Bessel functions. They, as well as the integral in Eqn. (11d), are tabulated in Ref. 11. A graphical representation of Eqn. (11d) is given in Fig. 11. It should be noted again that the asymptotic amplitude of $(1 + \pi/2)\cdot B_r$ for B(z) cannot be reached unless the material has a knee sufficiently far in the third quadrant of the $B_{//}(\mu_0 H_{//})$-curve.

REFERENCES

1. K. Halbach, NIM 169 (1980), 1

2) K.J. Strnat and G.I. Hoffer, Techn. Report, AFML-TR-65-446, Wright Paterson Air Force Base, (1966); J.B.Y. Tsui, D.J. Iden. K.J. Strnat and A.J. Evers, IEEE Trans. Magn. 2 (1972) p. 188.

3) K. Halbach, Proc. 1979 Particle Accelerator Conf., IEEE Trans. Nucl. Sci. NS-26 (1979) 3882.

4) M. McCaig, Permanent Magnets in theory and practice. (J. Wiley, London, 1977).

5) R.F. Holsinger and K. Halbach, Proc. 4 International Workshop on Rare Earth Cobalt Permanent Magnets (1979) p. 37.

6) R.F. Holsinger; Proc. of 1979 Linear Accel. Conf., Brookhaven, BNL-51134, p. 373.

7) N.V. Lazarev, S. Skachkov; Proc. of 1979 Linear Accel. Conf., Brookhaven, BNL-51134, p. 380.

8) R.L. Gluckstern, Proc. of this Conference.

9) R. Coisson; IEEE Transactions Vol. 24, No. 3, June 1977, p. 1681.

10) Unpublished internal report. A.S. Artamanov, et.al., Institute for Nuclear Physics, Novosibirsk.

11) Handbook of Mathematical Functions, edited by M. Abramowitz and I.A. Stegun. NBS Applied Mathematics Series No. 55; (1964).

*This work was supported by the U.S. Dept. of Energy under contract W-7405-ENG-48.

FIGURE CAPTIONS

Figure 1 – $B_{//}$ ($\mu_0 H_{//}$)-curve for REC.

Figure 2 – 2D cross-section of segmented REC quadrupole (beam in drawing plane).

Figure 3 – Cross-section through semi-infinite REC quadrupole (beam in drawing plane).

Figure 4 – REC quadrupole fringe field strength.

Figure 5 – Second derivative of REC quadrupole fringe field strength.

Figure 6 – 2D cross-section of linear REC undulator (beam in drawing plane).

Figure 7 – Cross-section through semi-infinite REC undulator (beam perpendicular to drawing plane).

Figure 8 – Fringe field strength of REC undulator.

Figure 9 – Strength of helical REC undulator.

Figure 10 – Periodic array of REC rings (beam in drawing plans).

Figure 11 – Field strength on axis of periodic array of REC rings.

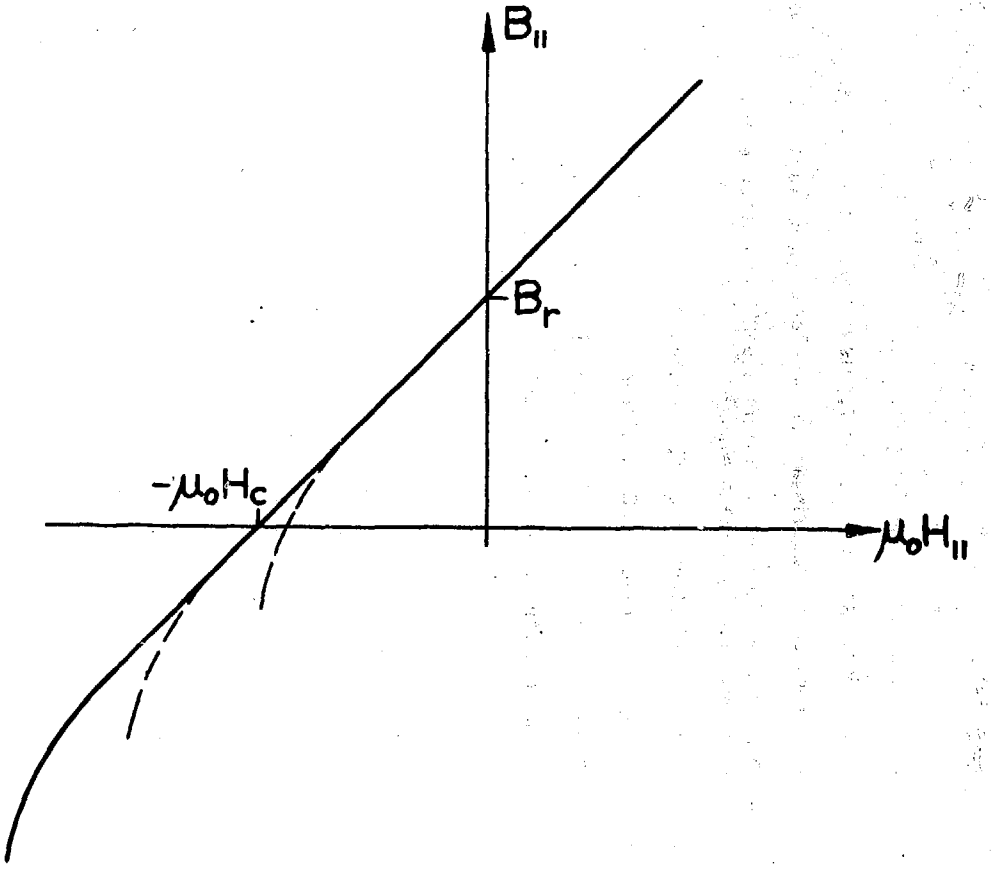

Figure 1

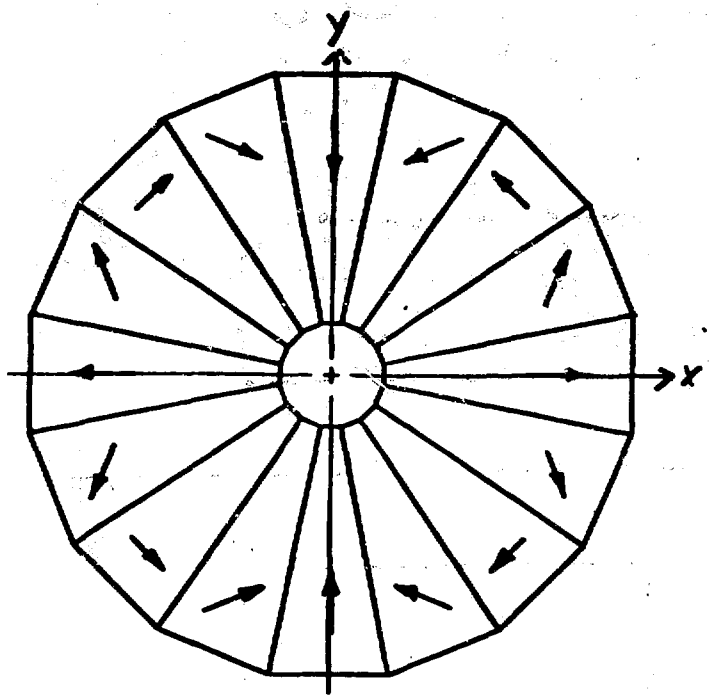

Figure 2

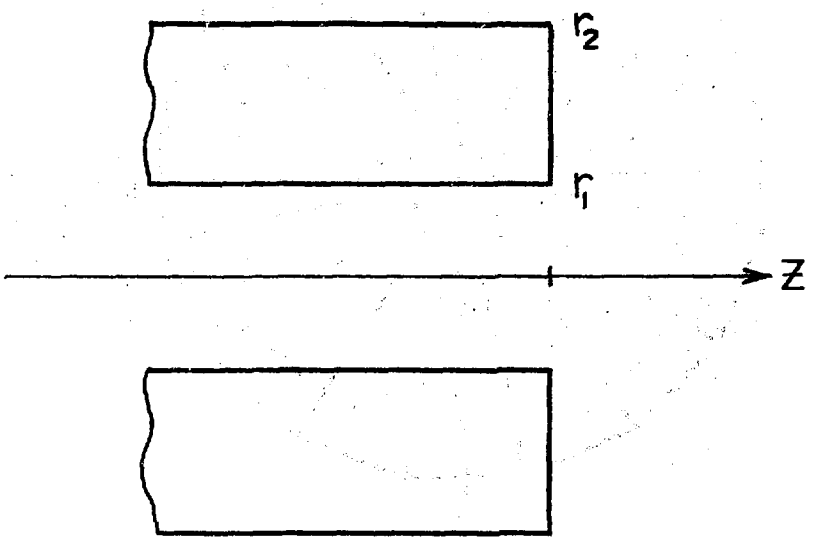

Figure 3

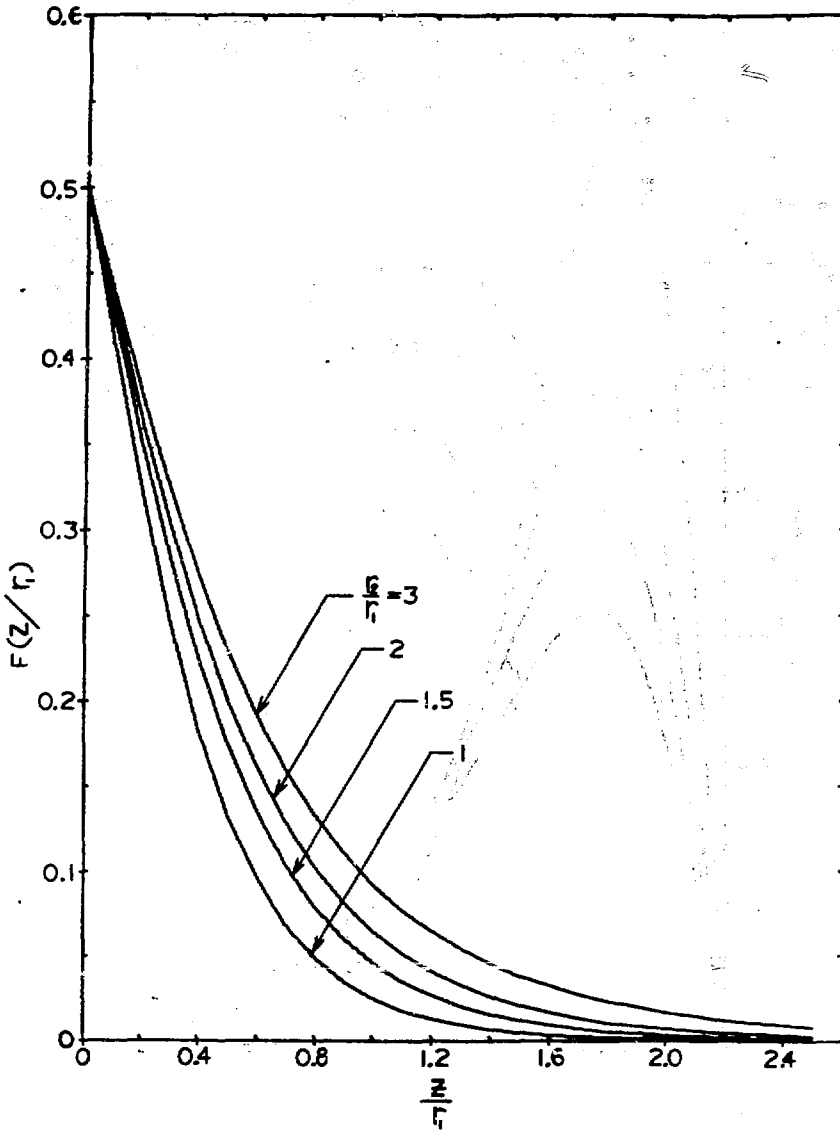

Figure 4

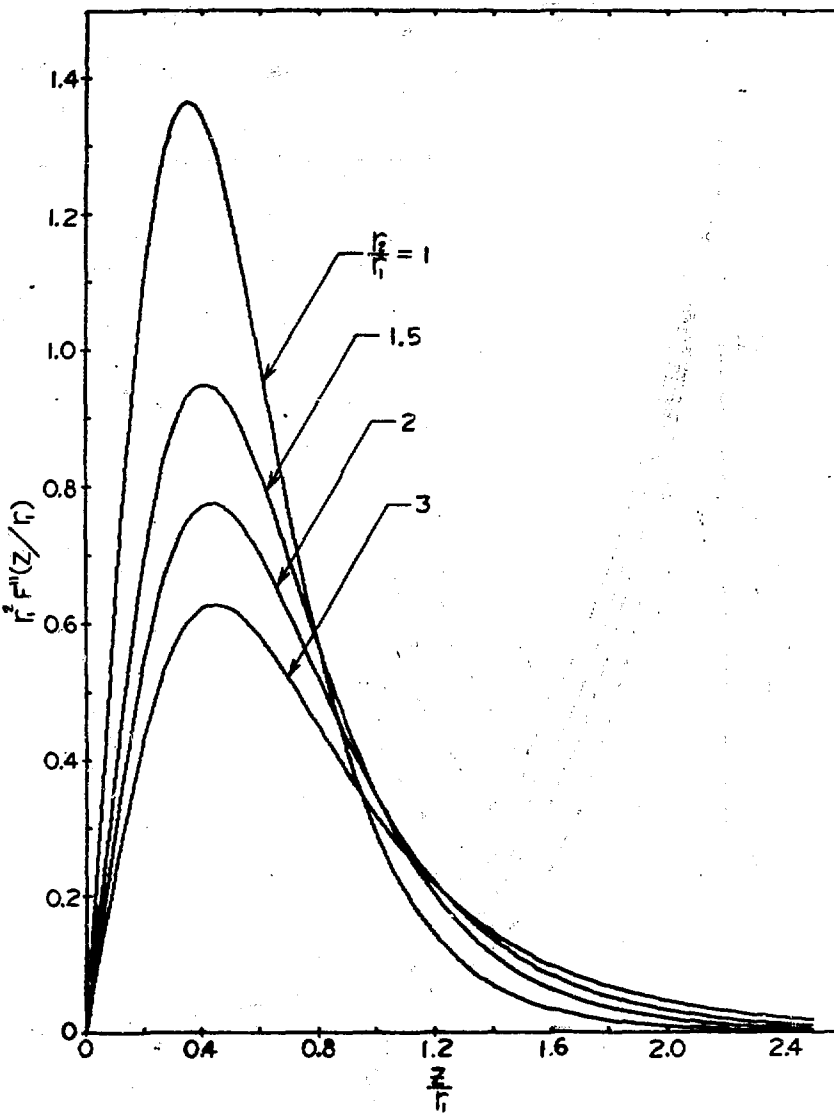
1.4
1.2
1.0
0.8
0.6
0.4
0.2
0
0
0.4
0.8
1.2
1.6
2.0
2.4
$\frac{r_2}{r_1} = 1$
1.5
2
3
$r_1^2 F''(Z/r_1)$
$\frac{Z}{r_1}$

Figure 5

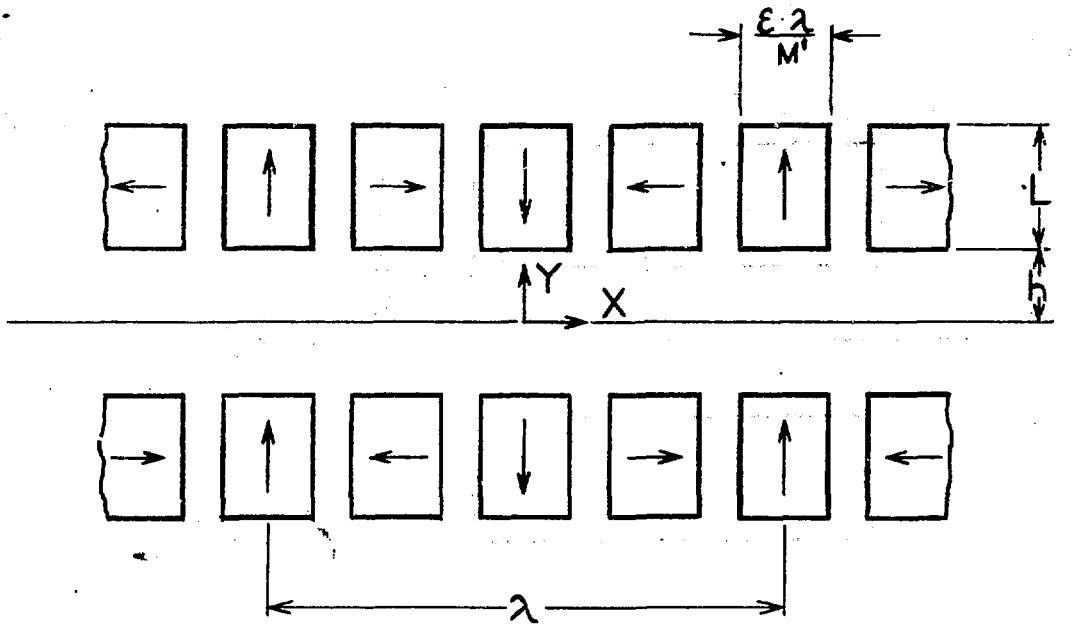

Figure 6

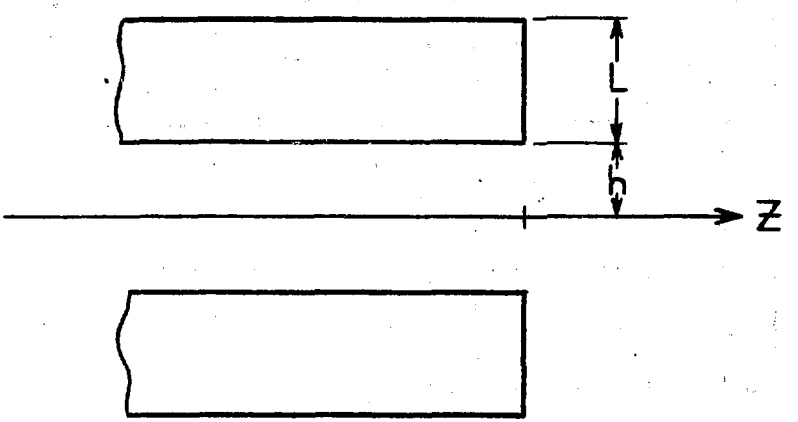

Figure 7

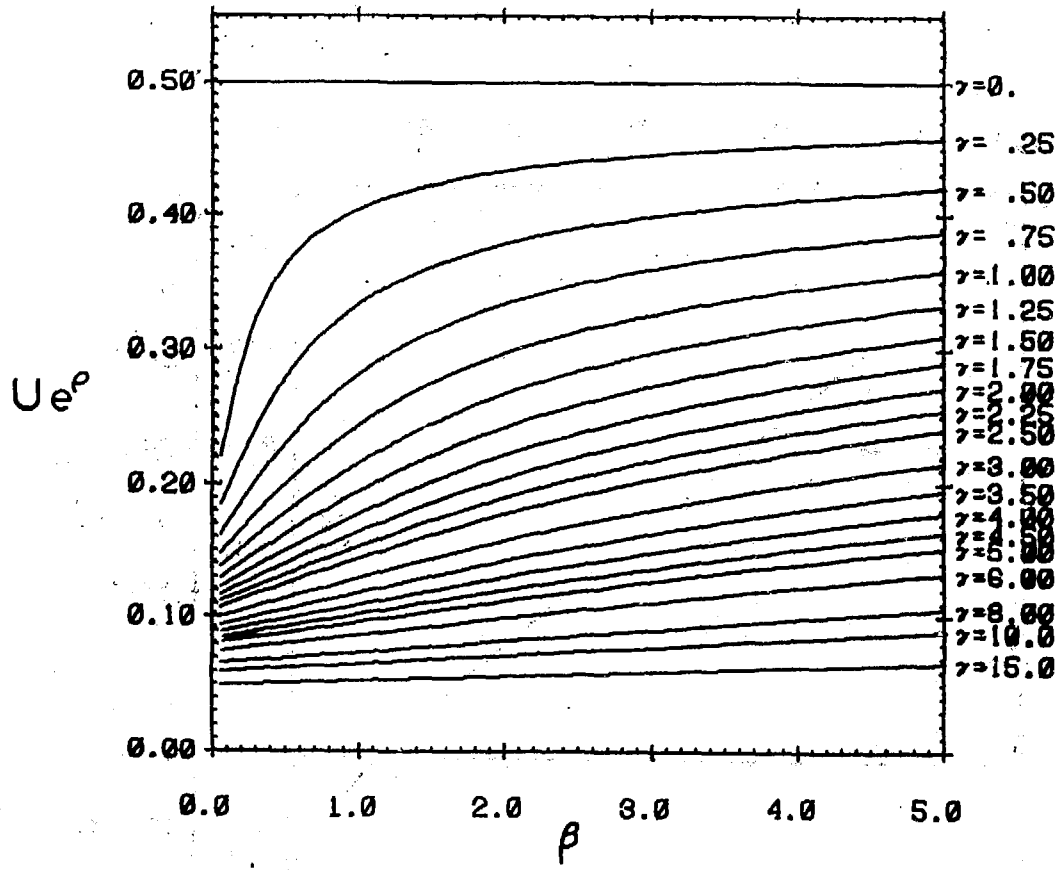
0.50
0.40
0.30
0.20
0.10
0.00
U_e^{ρ}
0.0
1.0
2.0
3.0
4.0
5.0
β
γ=0.
γ= .25
γ= .50
γ= .75
γ=1.00
γ=1.25
γ=1.50
γ=1.75
γ=2.50
γ=3.00
γ=3.50
γ=6.00
γ=10.0
γ=15.0

Figure 8

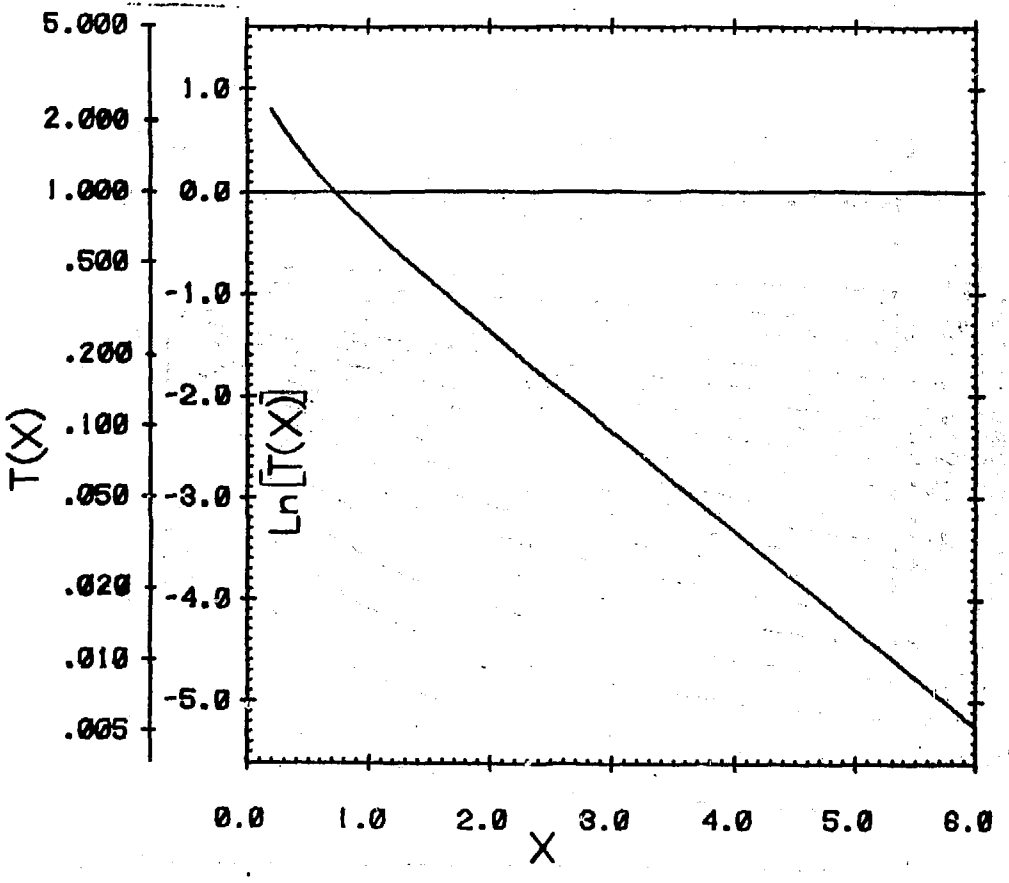
5.000
2.000
1.000
.500
.200
.100
.050
.020
.010
.005
T(X)
1.0
0.0
-1.0
-2.0
-3.0
-4.0
-5.0
Ln[T(X)]
0.0
1.0
2.0
3.0
4.0
5.0
6.0
X

Figure 9

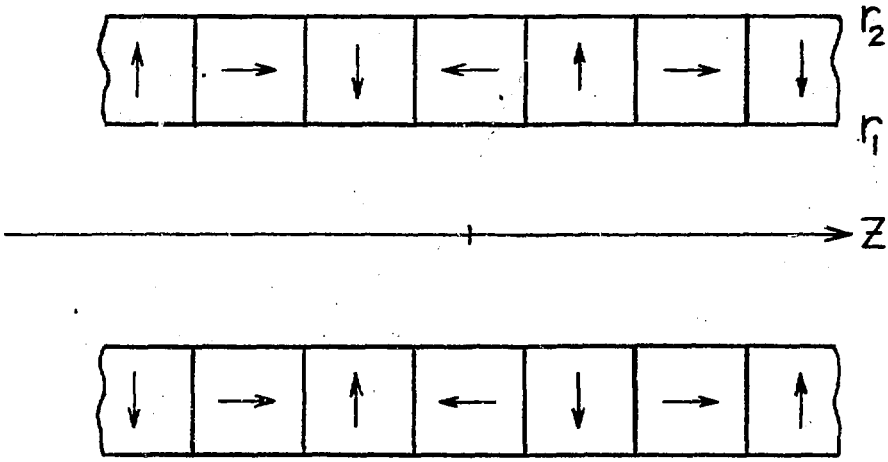

Figure 10

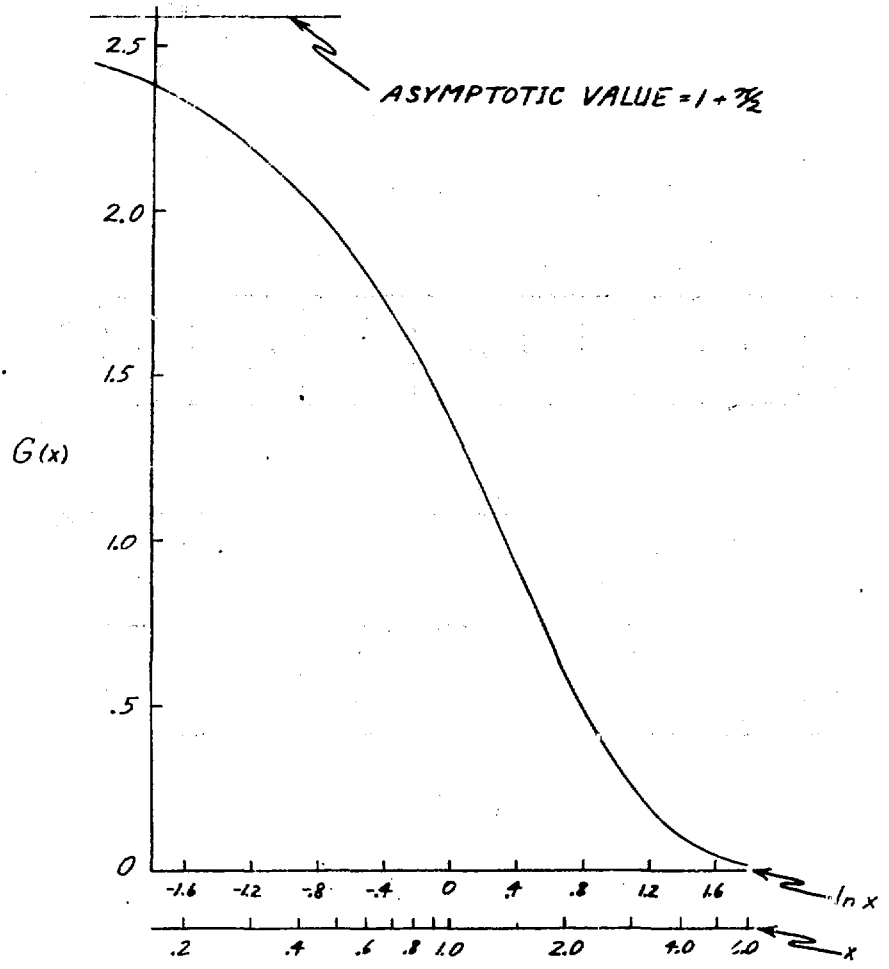

XBL 808-11001

Figure 11